Eng. & Technology, Vol.25, No.9, 2007

Reduced the Cooling Load and Improved Insulation Effect on Iraqi Buildings Using the Geothermal Energy Storage Phenomenon

Dr. Nazar Farag Antwan* Dr. Hassan K. Abdullah* Asslan M. M. Kamali*
Received on: 22/3/2007
Accepted on: 4/11/2007

Abstract

A numerical study has been done on Iraqi buildings (Baghdad) on 21st July to reduce the cooling load using a new system of geothermal energy. For this purpose, a flat vertical plate with high thermal conductivity extended into ground in 3 m deep used with eastern and southern walls construction.

The study shows that when using a plate only (without insulation) the cooling load is reduced by (13.2 %) and (12.7 %) for eastern and southern walls respectively. In addition, it shows that when using insulation at different arrangements the plate at the southern wall succeeds reduce in the cooling load by (8 %, 14.5% and 40 %) and (8 %, 15.8% and 41.3 %) at the eastern wall.

The study shows also that at some arrangements using flat plate with insulation, one can reach a very smooth cooling load distribution for southern and eastern walls, which gives a good and easy controlling of air temperature of the space. Also it can be seen from this study that the plate reduces the temperature of the walls outside surface especially when using insulation at the outside surface which means that the plate reduces the temperature and dissipats the thermal stresses which cause the cracks in the walls outside surface. The temperature reduction occurs in both walls at peak load, which means that the heat is dissipated to the ground.

As the inside, temperature of the wall surface has a great effect on the thermal comfort of occupants in the conditioned space and on the natural convection inside the space, when there is a good coincidence between the southern and eastern walls there will be a better thermal comfort. The plate also succeeded in making the inside surface temperature of the southern and eastern walls very close. The available experimental data from the literature for solar radiation, outdoor temperature and under-ground soil temperature gave a good agreement when compared with the theoretical results obtained from the used equations and programs in this research.

استخدام جديد لمنظومة طاقة الارض لتقليل حمل التبريد و تحسين اداء العازل في الابنية العراقية

الخلاصة

تم إجراء دراسة عددية للأبنية العراقيةِ (بغداد) في الحادي والعشرون من تموز لتَخفيض حمل التَبريد باستعمال نظام جديد للطاقة الناتجة من حرارة الأرض الجوفيةِ. لهذا الغرضِ تم مد صفيحة عمودية عالية التوصيلِ الحراري إلى عمق (3m) كجزء من التركيب البنائي للحائطين الشرقي والجنوبي .تظهر الدراسة أنّه عند استعمال الصفيحة فقط (بدون عزل) خفّضَ حمل التَبريد بنسب (13.2 %) و(12.7 %) للحائطِين الشرقي والجنوبي على التوالي. تظهر

* Dept. of Mechanical Eng., University of Technology, Baghdad-IRAQ.

https://doi.org/10.30684/etj.25.9.5
2412-0758/University of Technology-Iraq, Baghdad, Iraq

الدراسة أيضاً أنّه عند استعمال العزلِ الحراري في ترتيبات (مواضع) المختلفة من الحائطِ، نجحت الصفيحة لتَخفيض حملِ التَبريد للحائطِ الجنـــــوبي بنسب (8 %, 14.5% و40 %) و(8 %, 15.8% و41.3 %) للحائطِ الشرقي.تظهر الدراسةُ أيضاً انه في بَعْض الترتيباتِ وباستعمال الصفيحة مع العزلِ يُمْكِنُ أَنْ نَحصلَ على توزيع ناعم جداً (قليل التذبذب) لأحمال التبريدِ للحيطانِ الجنوبيةِ والشرقيةِ والذي يَعطينا سَيْطَرَة جيدة وسهلة على درجةِ الحرارة في تكييف الهواءِ. يُمْكِنُ أَنْ يُرى مِنْ هذه الدراسةِ أيضا أن الصفيحة نَجحتَ بتَخفيض درجةِ حرارة السطح الخارجي للجدار خصوصاً عند استعمال العزلِ عند السطح الخارجي مما يَعني أنّ الصفيحة تُخفّضُ درجةَ الحرارة وتمنع الإجهاد الحراريَ الذي يُسبّبُ الشقوقَ في السطح الخارجي للجدار، يَحْدثُ التَخفيض في درجةِ الحرارة في كلا الحائطين في الحمل الأقصى مما يَعني أنّ الحرارةَ فُرّقتْ إلى الأرض ولَنْ نَكُونَ مسؤولينَ عن التَعَامُل معها لاحقاً.بما أن درجةِ حرارة سطح الداخلي للجدار لها تأثير كبير على الراحة الحرارية للأشخاص الموجودين في الفضاء المكيّف وعلى معامل الانتقال الطبيعي للحرارة داخل ذلك الفضاءِ، لذلك عندما نَحصل على تقارب جيد مابين درجات الحرارة للأسطح الداخلية للجدران الأربعة فسنحصل على راحة حرارية أفضل داخل الحيّز المكيّف. لقد نَجحَت الصفيحة أيضاً في جَعْل درجةِ الحرارة للأسطح الداخلية للجدران الجنوبيةِ والشرقيةِ القريبةِ جداً. البيانات العملية (المأخوذة من وزارة العلوم و التكنولوجيا العراقية) للإشعاع الشمسي، درجة حرارة في الهواء الطلق ودرجة حرارة تربة أعماق الأرض أعطتْ تقارب جيد عند مُقارنْتها بالنَتائِج النظرية المستخرجة مِنْ المعادلات والبرامج المستعملة في هذا البحث.

Nomenclature

Symbol	mean	Unit
A	area	m^2
C	volumetric heat capacity	$J/m^3.K$
C_p	specific heat capacity	J/kg.K
d	declination	Degree
E	total emissive power	W/m^2
E_B	blackbody emissive energy	W/m^2
G	solar irradiation	W/m^2
g	acceleration of gravity	m/s^2
h	convective heat transfer coefficients	$W/m^2.K$
h	hour angle	Degree
k	thermal Conductivity	W/m.K
L	total width of the wall	m
l	latitude	Degree
N	number of day of the year	-
q	heat flux	W/m
R	thermal resistance	K/W
T	temperature	K, ˚C
t	time	Sec.
X	fraction factor	-
z	underground depth	m

z_{dp}	damping depth	m
Greek Letters		
α	thermal diffusivity	m^2/s
ά	absorptance	-
β	solar altitude angle	Degree
φ	solar azimuth angle	Degree
Φ	relative humidity	-
γ	wall solar azimuth	Degree
η	porosity	-
μ	stefan-Boltzmann constant	$W/(m^2.K^4)$
υ	ratio of volume	-
ρ	density	$kg.\ m^{-3}$
θ	volumetric moisture content	m^3/m^3
θ	angle of incidence	Degree
ζ	reflectivity	-
ψ	matrix potential	M
Ψ	sun's zenith angle	Degree
Є	emittance	-
τ	transmisivity	-
ω	frequency of a temperature fluctuation	Day^{-1}
Σ	angle of tilt	Degree

Subscript	
a	air
D	direct
d	diffuse
H	horizontal
k	critical
ℓ	liquid
ND	normal direct
om	organic matter
po	gas filled pores
q	quartz
R	reflected
s	solid, soil or surface
avg	average soil surface temperature.
amp-yr	amplitude of the annual temperature wave.
amp-day	amplitude of the daily temperature wave.

1- Introduction:

Geothermal energy has long been used for bathing, heating, and cooking since the beginning of recorded history. Low-temperature systems such as hot springs were used by the ancient Japanese, Greeks, and Romans, who enjoyed the recreational and therapeutic values of geothermally-heated spaces and bath houses Duffield, W., et.al.[1]. The geothermal heating and cooling system takes advantage of the fact that the ground a depth of several meters remain at a near constant temperature, so; in mid-winter it is warmer than the air, and in mid-summer it is cooler Lund J. W., et.al. [2]. Shen L.S. and Ramsey J.W., 1988 [3] developed a two-dimensional finite difference numerical model to study coupled soil heat and moisture flow around an earth-sheltered construction. Simulations of a basement wall backfilled with sand and a clay loam were performed. Deru, M., 2003 [4] investigated the ground-coupled heat and moisture transfer from buildings, and developed results and tools to improve energy simulation of ground-coupled heat transfer. He found that basement walls are sensitive to the conditions (temperature and humidity) at the surface. Basement floors are relatively unaffected by short-term variations at the surface, but they are closely tied the deep ground conditions. Compared winannual simulations from the heat-and-moisture-transfer model the heat-transfer model produced agreeable results when an appropriate value for soil thermal properties was chosen. The value of the solar irradiation at the surface of the earth on a clear day is given by ASHRAE Handbook [5, 6]. There are many workers dealing with how to determine the temperature distribution in the soil due to heat flow in the soil Takakura T., Jordan, et.al. [7], Davies J.B. [8] and Novak M.D. [9], consider that the thermal conductivity does not change with temperature. Other workers take into consideration the variation thermal conductivity in the soil Sepaskhah A.R.et.al. [10] and Eshel A. et.al.[11]. Wierenga P.J. et.al.[12] suggest models to calculate the underground temperature by measuring the temperature change at the soil surface and the thermal diffusivity which depends on the soil depth and its temperature. Data from Milly P.C.D. [13] on simultaneous heat and mass transfer in one-dimensional soil samples indicate that the temperature distribution is not strongly dependent upon moisture content in the particular unsaturated soil used. Most previous studies were for one-dimensional vertical flow region.

In this research a high conductive material (aluminum or copper) flat plate is used as one of the exterior walls layers, but this flat plate is extended downward into the ground (for a certain depth). Its job is to work as a heat dissipater (the upper part) and heat exchanger (the underground part), since it has a higher thermal conductivity than the other building materials, a part of the energy absorbed by the upper part will be exchanged with ground soil (which is at lower temperature) and the building cooling load would be reduced, Fig. (14) shows the case study presented in this work. For more details about the present work see Aslan [20].

2-Theory

Heat transfer is energy in transient, which occurs as a result of a temperature gradient or difference. This temperature difference is thought of as a driving force that causes heat to flow. Heat transfer occurs in three basic mechanisms or modes: conduction, convection, and radiation. The key to maintaining a comfortable temperature in a building is to reduce the heat transfer out of the building in the winter and reduce heat transfer into the building in the summer, Novak M.D. [9].The flow of heat through porous media such as soils can be important for many engineering structures. The two major modes of energy transfer in soils are conduction and convection. It has been found that the relative proportions of these modes of energy transfer are a function of grain size, with conduction occurring predominantly in fine-grained soils and convection in coarse-grained soils, Farouki, O.T. [19]. The Fourier's law of conduction, ASHRAE Handbook [5] is

$$q' = -kA\frac{dT}{dx} = \text{rate of heat transfer} \quad (1)$$

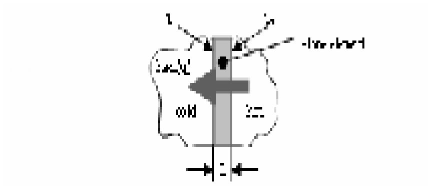

Figure (1) Heat flow through plane element

For heat flow through a wall Fig. (1);

$$q' = -kA\frac{(T_2 - T_1)}{L}, q = q'.t \quad \dots(2)$$

The three-dimensional conduction equation in Cartesian Coordinates is derived by taking a control volume element. Appling the first law of thermodynamics to the element, we get:

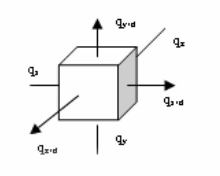

Figure(2)

$$q''' = -k\left[\frac{\partial^2 T}{\partial x^2} + \frac{\partial^2 T}{\partial y^2} + \frac{\partial^2 T}{\partial z^2}\right] + \frac{1}{\alpha}.\frac{\partial T}{\partial t} \quad (3)$$

For the case we have (2-D with no heat generation) equation (3) would be;

$$k\left[\frac{\partial^2 T}{\partial x^2} + \frac{\partial^2 T}{\partial y^2}\right] = \frac{1}{\alpha}.\frac{\partial T}{\partial t} \quad \text{------ } (4)$$

Using numerical analysis to solve Eq. (4) and choosing central finite difference formation, and assuming that (dx=dy); yield

$$T_{i,j}^{n+1} = \frac{a.dt}{dx^2}\left(T_{i+1,j}^n + T_{i-1,j}^n + T_{i,j+1}^n + T_{i,j-1}^n\right) + \left(1 - \frac{4.a.dt}{dx^2}\right)T_{i,j}^n \quad (5)$$

Convection is the mode of heat transfer between a solid surface and the adjacent fluid that is in motion, and it involves the combined effects of conduction and fluid motion. It can be obtained from-

$$q' = h.A.(T_W - T_\infty) \quad \text{---- } (6)$$

The total irradiation G_t on a surface normal to the sun's rays is made up of normal direct irradiation G_{ND}, diffuse irradiation G_d, and reflected irradiation G_R are given by [5]

$$G_t = G_{ND} + G_d + G_R \quad ----(7)$$

Neglecting the coupling of water transfer in the soil with the heat transfer, Wang S.K. [15], we can assume the following Fourier law of diffusion to govern the soil heat transfer;

$$(\rho C_p)_s \frac{\partial T}{\partial t} = \frac{\partial}{\partial z}\left[k\frac{\partial T}{\partial z}\right] + \frac{\partial}{\partial x}\left[k\frac{\partial T}{\partial x}\right] \quad (8)$$

At the ground-surface the temperature is a function of time (days of year N) and the time of a day (hours), the governing equation is;

$$T_s = T_{avg} + T_{amp-yr}\sin\left(\frac{2p\,(N-N_{ref})}{365}\right) + T_{amp-day}\sin\left(\frac{2p\,(t-t_{ref})}{24}\right) \quad (9)$$

Note; N_{ref} , and t_{ref} are time lags from an arbitrary date and time (Jan. 1st, 12 p.m) to the date and time at which $T_s=T_{avg}$, and they are taken to be N_{ref}=105 (April 15th), t_{ref}=15 (3 p.m), Cruse R.M. [18].

While the underground soil initial temperature is a function of depth and time;

$$T(z,t) = T_{avg} + T_{amp-yr}\exp(-z/z_{dp}).\sin\left(\frac{2p\,(N-N_{ref})}{365} - (z/z_{dp})\right) \quad (10)$$

The dampening depth (z_{dp}) is the depth where the variations in soil temperature are 1/e = 0.368 times the temperature variations at the soil surface. The dampening depth is a function of the soil's thermal properties as well as the period of variation considered, ASHRAE Handbook [6];

$$z_{dp} = \sqrt{\frac{2\alpha}{\omega}} \quad ---(11)$$

where ω is the frequency of a temperature fluctuation. For annual fluctuation ω =2π/365 . Note that the dampening depth is 19 times greater for annual variations than it is for daily variations [18]. The daily dampening depth, according to [6] for saturated soil is 12.2 cm and for an annual dampening depth, 233 cm.

To predict heat transfer in soil under the conditions of steady and non-steady heat flow requires the knowledge of the basic thermal properties of soil, Noborio K. [17].

The model for the soil thermal conductivity is taken from, De Vries D.A. [16]. And it can be determined using Eq. (12).

$$k = \frac{x_w k_w + \xi_{po} x_{po} k_{po} + \sum_{i=1}^{n} \xi_i x_i k_i}{x_w + \xi_{po} x_{po} + \sum_{i=1}^{n} \xi_i x_i} \quad (12)$$

The volumetric heat capacity C (J/m^3·K) is calculated as a weighted average of the specific heat capacities C_p (J/kg·K) of the soil constituents as shown in Eq. (13), the heat capacity of the gases is neglected [14];

$$C = x_w \rho_w C_{p_w} + \sum_{i=1}^{n} x_i \rho_i C_{p_i} \quad ---(13)$$

There are some cases (nodes) which need a special equations to describe the flow of heat passing through. Considering a point P that is assumed to be the intersection point of four different materials (Fig 3) ;

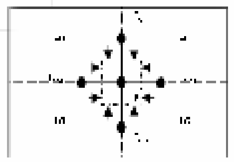

Figure(3) Node among four different matrieals

$$T_{i,j}^{n+1} = \frac{2.dt}{dx^2}\left[\begin{array}{l}(a_2+a_3).T_{i+1,j}^n + (a_1+a_4).T_{i-1,j}^n \\ +(a_1+a_2).T_{i,j-1}^n + (a_3+a_4).T_{i,j+1}^n\end{array}\right]$$

$$+\left[1-\frac{4.dt}{dx^2}(a_1+a_2+a_3+a_4)\right].T_{i,j}^n \quad \text{---(14)}$$

where;

$$a_1 = \frac{k_1}{\rho_1.C_1+\rho_2.C_2+\rho_3.C_3+\rho_4.C_4},$$

$$a_2 = \frac{k_2}{\rho_1.C_1+\rho_2.C_2+\rho_3.C_3+\rho_4.C_4},$$

$$a_3 = \frac{k_3}{\rho_1.C_1+\rho_2.C_2+\rho_3.C_3+\rho_4.C_4},$$

$$a_4 = \frac{k_4}{\rho_1.C_1+\rho_2.C_2+\rho_3.C_3+\rho_4.C_4}$$

For P that is assumed to be the intersection point of two different materials (Fig. 4) ;

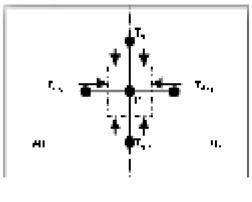

Figure (4) Node between different materials

$$T_{i,j}^{n+1} = \frac{2.dt}{dx^2}\left[\begin{array}{l}(a_2).T_{i+1,j}^n + (a_1).T_{i-1,j}^n \\ +\frac{1}{2}(a_1+a_2).(T_{i,j-1}^n + T_{i,j+1}^n)\end{array}\right]$$

$$+\left[1-\frac{4.dt}{dx^2}(a_1+a_2)\right].T_{i,j}^n \quad \text{---(15)}$$

where;

$$a_1 = \frac{k_1}{\rho_1.C_1+\rho_2.C_2},$$

$$a_2 = \frac{k_2}{\rho_1.C_1+\rho_2.C_2}$$

Considering a point P that is assumed to be the intersection point of two different materials and insulated surface (Fig. 5) ;

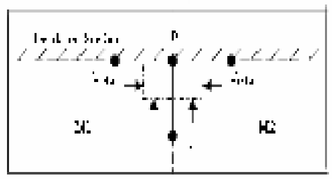

figure (5) Node between two different materials and insulated surface

$$T_{i,j}^{n+1} = \frac{2.dt}{dx^2}\left[\begin{array}{l}(a_2).T_{i+1,j}^n + (a_1).T_{i-1,j}^n \\ +(a_1+a_2).T_{i,j-1}^n\end{array}\right]$$

$$+\left[1-\frac{4.dt}{dx^2}(a_1+a_2)\right].T_{i,j}^n \quad \text{---}\quad (16)$$

where;

$$a_1 = \frac{k_1}{\rho_1.C_1+\rho_2.C_2},$$

$$a_2 = \frac{k_2}{\rho_1.C_1+\rho_2.C_2}$$

Considering a point P that is assumed to be the intersection point of three different materials (Fig. 6) ;

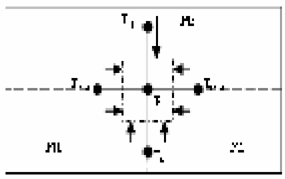

figure (6) Node among three different materials

$$T_{i,j}^{n+1}=\frac{2.dt}{dx^2}\left[\begin{array}{l}(a_2+a_3).T_{i+1,j}^{n}+(a_1+a_3).T_{i-1,j}^{n}\\+(a_1+a_2).T_{i,j-1}^{n}+(2.a_3).T_{i,j+1}^{n}\end{array}\right]$$

$$+\left[1-\frac{4.dt}{dx^2}(a_1+a_2+2.a_3)\right].T_{i,j}^{n} \qquad (17)$$

where;

$$a_1=\frac{k_1}{\rho_1.C_1+\rho_2.C_2+2.\rho_3.C_3},$$

$$a_2=\frac{k_2}{\rho_1.C_1+\rho_2.C_2+2.\rho_3.C_3},$$

$$a_3=\frac{k_3}{\rho_1.C_1+\rho_2.C_2+2.\rho_3.C_3}$$

For external surface with convection subjected to it (Fig. 7);

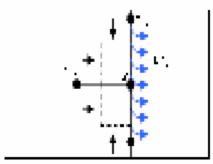

figure (7) Node on the external surface with convection

$$T_{i,j}^{n+1}=\frac{2a.dt}{dx^2}\left(\begin{array}{l}T_{i-1,j}^{n}+\frac{1}{2}T_{i,j+1}^{n}+\frac{1}{2}T_{i,j-1}^{n}\\+\frac{h_{in}.dx}{k}T_{in}\end{array}\right)$$

$$+\left(1-\frac{2.\alpha.dt}{dx^2}(2+\frac{h_{in}.dx}{k})\right)T_{i,j}^{n} \qquad --(18)$$

For an external surface with convection and heat flux subjected to it (Fig. 8) ;

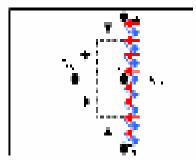

Figure (8) Node on the external surface with convection and heat flux

$$T_{i,j}^{n+1}=\frac{2a.dt}{dx^2}\left(\begin{array}{l}T_{i-1,j}^{n}+\frac{1}{2}T_{i,j+1}^{n}+\frac{1}{2}T_{i,j-1}^{n}\\+\frac{h_{out}.dx}{k}T_{out}\end{array}\right)$$

$$+\left(1-\frac{2.a.dt}{dx^2}(2+\frac{h_{out}.dx}{k})\right)T_{i,j}^{n}+ \qquad (19)$$

$$\frac{dx}{k}.\frac{2a.dt}{dx^2}.q''$$

Considering a point P that represented an external corner point with two insulated sides (Fig. 9)

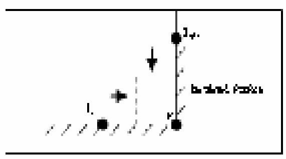

Figure (9) Insulated external corner node

$$T_{i,j}^{n+1}=\frac{2.a.dt}{dx^2}\left(T_{i-1,j}^{n}+T_{i,j+1}^{n}\right)+$$

$$\left(1-\frac{4.a.dt}{dx^2}\right)T_{i,j}^{n} \qquad --(20)$$

Consider point P as an external corner point with one insulated side and a heat flux subjected to the other (Fig. 10) ;

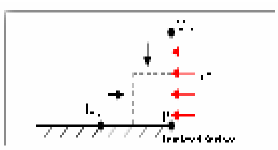

figure (10) External corner node with one side heat flux

$$T_{i,j}^{n+1} = \frac{2.a.dt}{dx^2}\left(T_{i-1,j}^{n} + T_{i,j+1}^{n} + \frac{dx}{k}q''\right) \quad (21)$$
$$+\left(1-\frac{4.a.dt}{dx^2}\right)T_{i,j}^{n}$$

Consider point P as an external corner point with one insulated side and convection subjected to the other (Fig. 11);

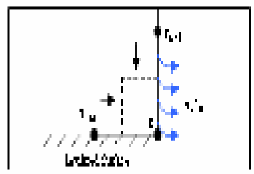

Figure (11) external corner node with one side convection

$$T_{i,j}^{n+1} = \frac{2.a.dt}{dx^2}\left(T_{i-1,j}^{n} + T_{i,j+1}^{n} + \frac{h.dx}{k}T_o\right) \quad (22)$$
$$+\left(1-\frac{2.a.dt}{dx^2}.\left(2+\frac{h.dx}{k}\right)\right)T_{i,j}^{n}$$

Consider a point P that is a external corner point with one insulated side and the other is subjected to convection and heat flux (Fig.12);

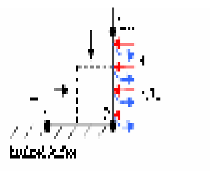

Figure (12) external corner node with one side subjected to convection and heat flux

$$T_{i,j}^{n+1} = \frac{2.a.dt}{dx^2}\left(T_{i-1,j}^{n} + T_{i,j+1}^{n} + \frac{dx}{k}.q'' + \frac{h.dx}{k}T_o\right)$$
$$+\left(1-\frac{2.\alpha.dt}{dx^2}.\left(2+\frac{h.dx}{k}\right)\right)T_{i,j}^{n} \quad --(23)$$

Cases study

In this study we take an Iraqi wall that is constructed of cement, brick, and gypsum with vertical plate (having high thermal conductivity) integrated with wall construction and extended down in the ground for 3 meters. Many construction arrangements as shown in Figure (13) are studied to find out the best arrangement which gives lower cooling load and uniform distribution. Table (1) shows the thermal properties of the wall materials and Table (2) shows thermal properties and densities of soil materials, water and air at 10°C.

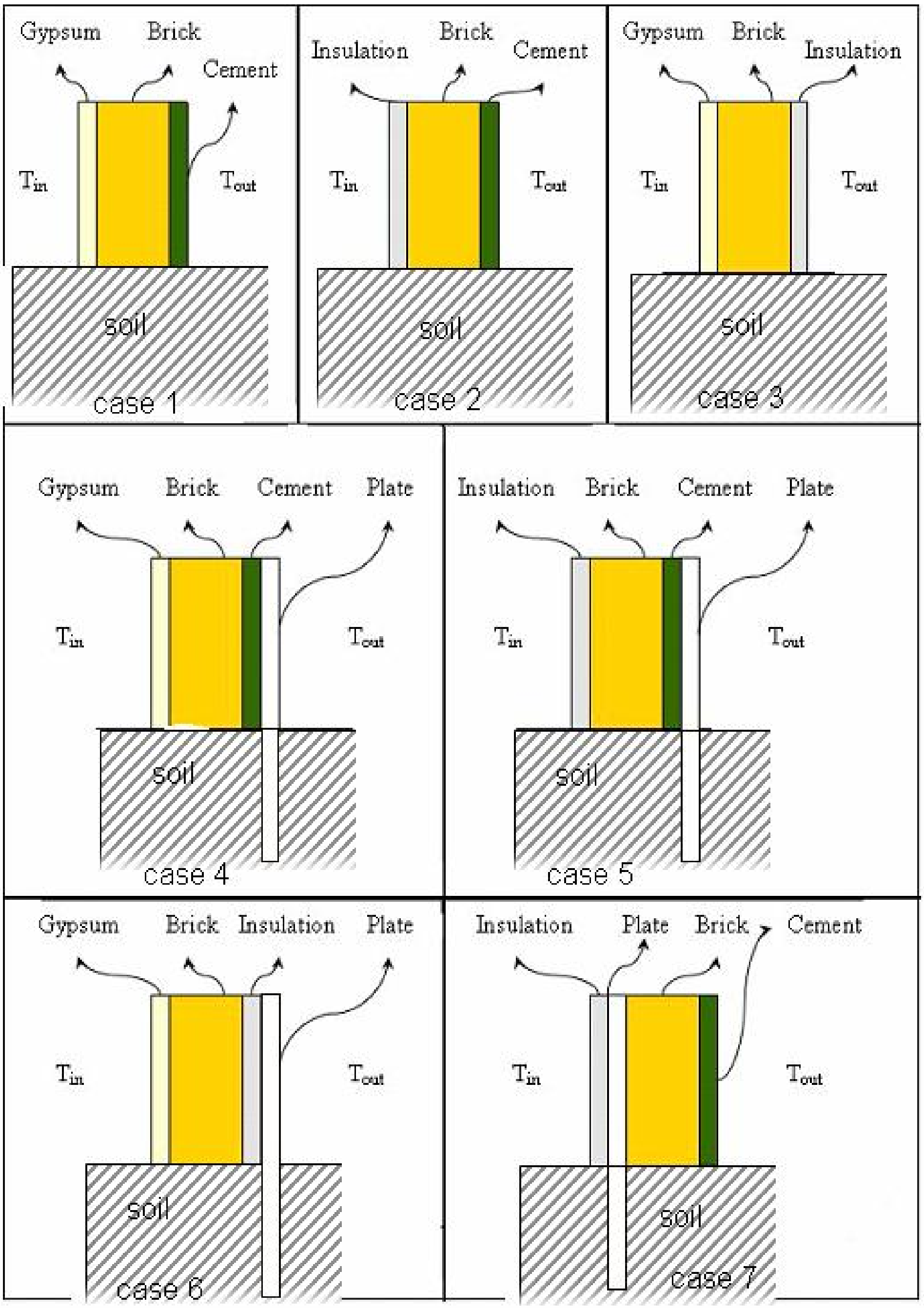

Figure (13) Wall arrangements

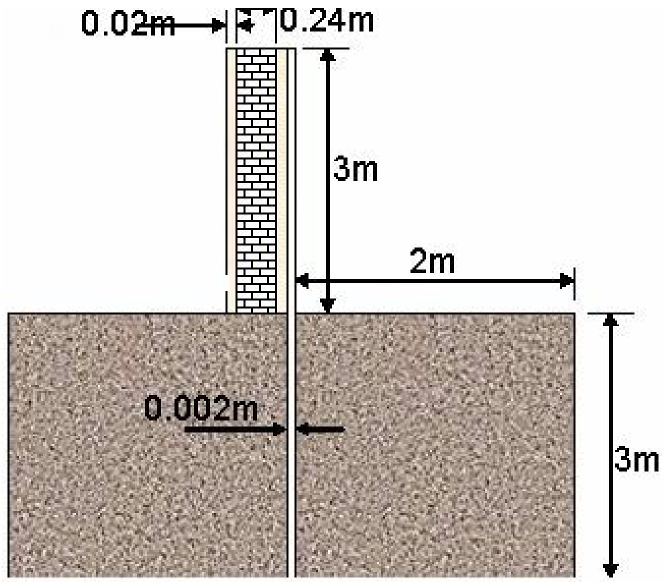

Figure (14) Sketch for case study

Table (1) Thermal properties of the wall materials

Material properties	Thermal conductivity (W/m.K)	Density (kg/m^3)	Heat capacity (J/kg.K)
Gypsum	0.47	1680	1085
Brick	0.72	1920	835
Cement	0.72	1860	1085
Aluminum	237	2700	903
Insulation	0.04	91	840

Table (2) Thermal properties and densities of soil materials, water and air at 10°C.

Substance	ρ (kg / m³)	C_p (J / kg . K)	k (W / m . K)
Quartz	2.66×10^3	752	8.8
Organic Matter	1.3×10^3	1923	0.25
Other Minerals	2.65×10^3	755	2.9
Water	1.0×10^3	4.2×10^3	0.57
Air	1.25	1000	0.025

3 Results and discussion

In all cases it is obvious that a reduction in the heat flow inside the air-conditioned space takes place. Figs.(15, 16) show that the insulation and the plate reduce the cooling load and does not change its distribution (cases 2, 3, 4), and when is used the insulation with plate the load reduces and its distribution changes. Also from these figures one can see that the arrangement of the plate and the insulation affects the reduction in the cooling load and its distribution. These figures show that case (6) gives uniform load in the eastern and southern walls and case (7) gives more reduction in the cooling load but not uniform as case (6). Figs. (17, 18) represent the outside temperatures of the eastern and the southern walls, and when comparing case (3) and case (6) one can see that the plate success in reducing the temperature that increased when using insulation at on outside surface. Also from these figures one can see that the efficiency of the plate increases as the temperature of the wall surface increases, and for this reason the plate at the eastern wall reduces the temperature more than at the southern wall.

For the normal wall (case 1) the inside surface temperature is varying. The temperature distribution at the inside surface of the two walls (Figs. 19 and 20) is to very similar to the heat passing through distribution system with a maximum value at (12 P.M) and a minimum value at (12 A.M) for the southern wall and a maximum value at (10 P.M) and a minimum value at (10 A.M) for the eastern wall. Through day time between (31 and 33˚C) for the southern wall and between (32 and 34.5˚C) for the eastern wall, which leads to non-homogenous temperature distribution inside the room and uncomfortable condition for people inside it. While for case (7) the variation is amount is less than 1˚C for both south and east oriented walls. The temperature of the inside surface of the eastern wall is higher than that of the southern wall with; 1˚C for cases 2,3,4,5 and 6, while for case (7) the temperature difference drops to 0.5˚C which gives a better condition of human comfort. From the same figures it can be seen that when which is placed close to the inside surface affects the temperature distribution and gives good results. Figures (21and 22) show the temperature difference between the average temperatures of the upper and lower parts of the plate for each hour and for four cases. The high fluctuation in the temperature difference for the case is due to the position of the plate on the outside surface of the wall which made the upper part of the plate highly and quickly effective by the changes in the outdoor conditions while the lower part of the plate remains approximately at the same average temperature due to the effect of the surrounding soil. In case (7) the plate is positioned near the inside surface of the wall with an insulation material right after it, this position made the plate less affected by the changes of the outdoor conditions and helped to maintain a certain amount of temperature difference between the two parts. Fig. (23) shows the total heat passing-in for the entire day (24 hours) for each case. From this figure it can be seen that when using insulation as an inner layer of the wall, cases (2,5 and 7), the plate in case (5) reduces the cooling load by (8 %) compared with case (2) (for both southern and eastern walls) but in case (7) the plate reduces the cooling load by (40% and 41.3 %) compared with case (2) (for southern and eastern walls respectively). And when using insulation as an outer layer of the wall, cases (3 and 5), the plate reduces the cooling load by (14.5% and 15.8 %). This figure shows that the plate is more effective in such arrangement than the others.

References:-

[1] Duffield, W., and J.H. Sass, "Geothermal Energy – Clean Power From the Earth's Heat". U.S. Geological Survey Circular, No. 1249. 2003

[2] Lund, J.W., Freeston, D.H. and Boyed T.L., 2005. "world-wide direct utilization of geothermal energy". In; Proceedings of the World Geothermal Congress 2005. Paper Number: 0007. 2005

[3] Shen L.S. and Ramsey J.W., 1988."An investigation of transient, two-dimensional coupled heat and moisture flow in the soil surrounding a basement wall". International Journal of Heat and Mass Transfer. Vol.31, No.7, pp. 1517-1527, 1988.

[4] Deru, M., "A Model for Ground-Coupled Heat and Moisture Transfer from Buildings". National Renewable Energy Laboratory**,** NREL/TP-550-33954. Golden, Colorado 80401-3393. Prepared under Task No. BEC3.4005, June 2003.

[5] ASHRAE Handbook, Fundamentals Volume, American Society of Heating, Refrigerating and Air Conditioning Engineers, Inc., Atlanta, GA, 1989.

[6] ASHRAE, "Fenestration", Chapter 27 Handbook of Fundamentals, New York, NY, 1981.

[7] Takakura T., Jordan K.A. and Boyed I.L. "Dynamic simulation of plant growth and environment in green house". Trans. ASAE 14: 964-971. 1971.

[8] Davies J.B. "Simulation of heat and moisture movement during drying of a two-dimensional soil profile". Ph.D. Diss. Clemson Univ., Clemson, Sc. Diss. Abstr (DDK77-29688). 1977.

[9] Novak M.D. "Analytical solutions for two-dimensional soil heat flow with radiation surface boundary conditions". Soil Sci. Soc. Am. J. 57: 30-39. 1993.

[10] Sepaskhah A.R. and Boersma L. "Thermal conductivity of soils as a function of temperature and water content". Soil Sci. Soc. Am. J. 43: 439-444. 1979.

[11] Eshel A. and Curry R.B. "Soil moisture and soil heat simulator". Agricultural engineering series 103, Ohio Agricultural Research and Development Centre. 1980

[12] Wierenga P.J. and de Wit C.T. "Simulation of heat flow in soils". Soil Sci. Soc. Am. Proc. 43: 845-848. 1970

[13] Milly P.C.D. and Eagleson P.S., "The coupled transport of water and heat in a vertical soil column under atmospheric excitation". Tech. Rep. 258. R.M. Parsons Lab., Dept. of Civil Eng. Mass. Inst. Of Technol. Cambridege. 1980

[14] Savvidou, C.,. "Centrifuge modelling of heat transfer in soil". Centrifuge 88, Balkema, Rotterdam, p. 583-591. 1988

[15] Wang S.K., "Handbook of Air Conditioning and Refrigeration". Second Edition, Includes INDEX; Isbn 0-07-068167-8. Th7687.W27, 2000.

[16] De Vries, D.A. and Van Wijk, W.R. "Thermal Properties of Soils." Physics of Plant Environment. Amsterdam: North-Holland Publishing Company 1966..

[17] Noborio K., McInnes K.J., Heilman J.L.: "Two-dimensional model for water, heat, and solute transport in furrow-irrigated soil: I. Theory, II Field evaluation". Soil Sci. Soc. Am. J., 60, 1001-1021, 1996.

[18] Cruse R.M., "Modelling tillage effects on soil temperature, physical properties and processes". Spec. Pub. No. 44, Am. Soc. Of Agron., Inc., Madison, Wisconsin 1982.

[19] Farouki, O.T., "Thermal Properties of Soils." CRREL Monograph 81-1. U.S. Army Cold Regions Research and Engineering Laboratory, Hanover, NH. 1981

[20] Asslan." Numerical Study of a New Geothermal System to Reduce Cooling Load in Iraqi Buildings". 2007

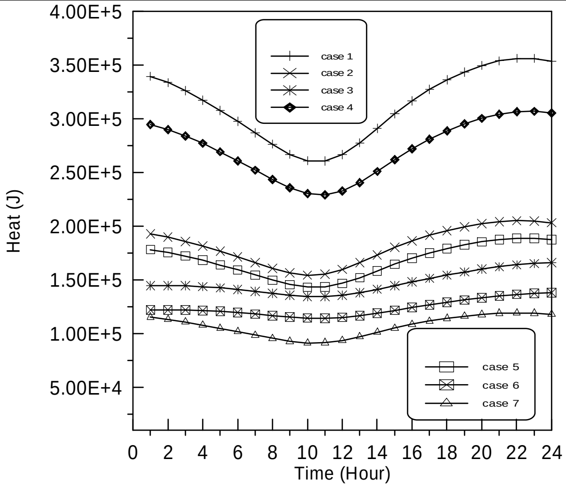

Figure (15) Heat flow through the easteran wall

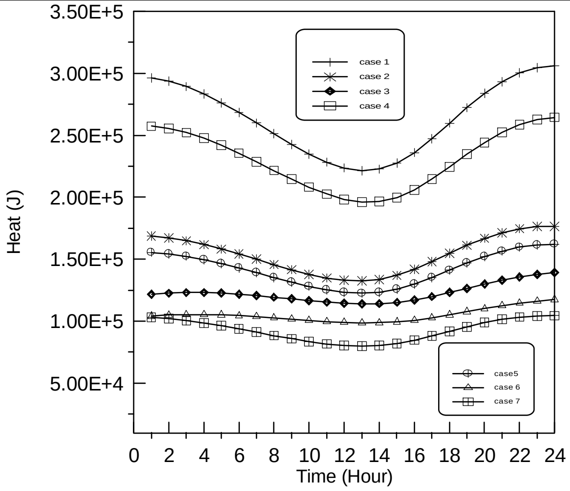

Figure (16) Heat flow through the southren wall

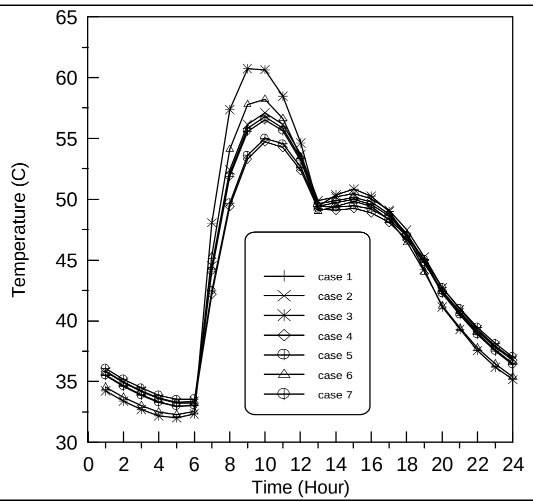

Figure(17) Outside surface temperature for eastern wall

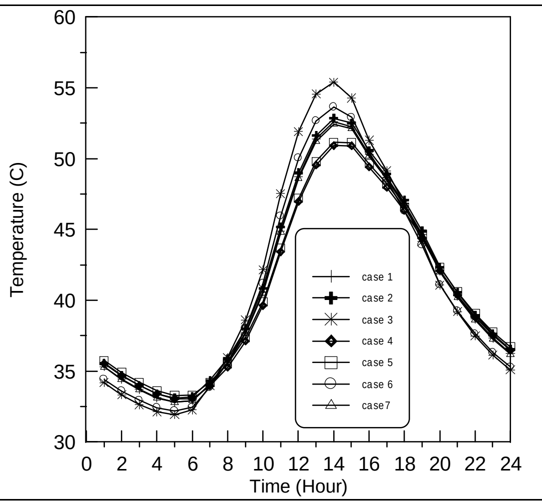

Figure (18) Outside surface temperature for eastern wall

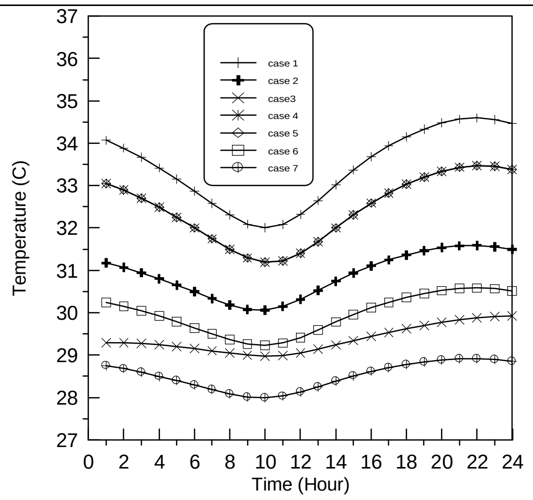

Figure(19) Inside surface temperature for eastern wall

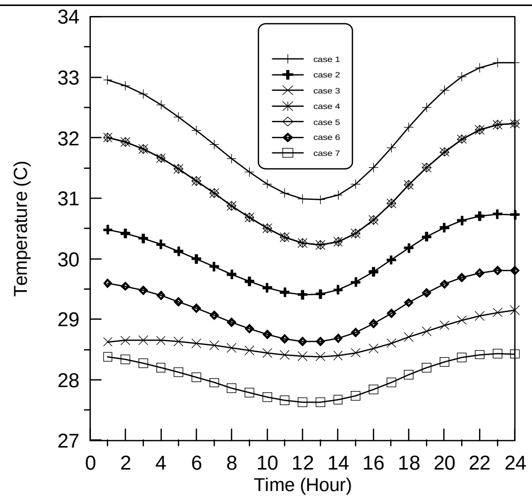

Figure (20) Inside surface temperature for southeren wall

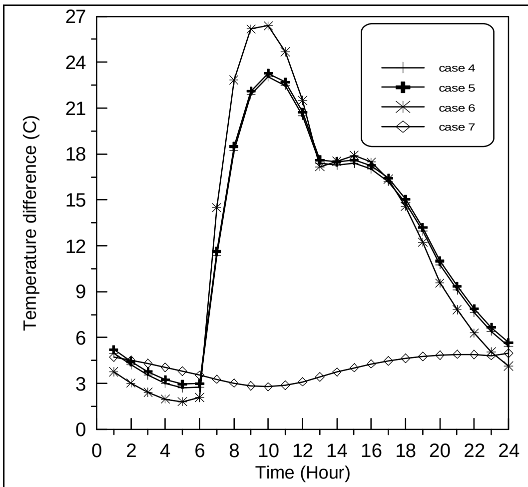

Figure (21) Temperature difference between the upper and lower parts of the plate for eastern wall

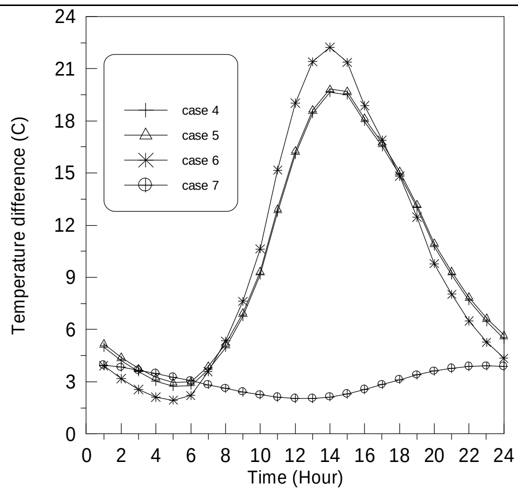

Figure (22) Tempereture difference between the upper and the lower parts of the plate for southern wall

Table (3) Total heat for the different cases considered in this work

case	total heat flow from S wall (kJ)	total heat flow from E wall (kJ)
1	6324.966	7506.412
2	3692.236	4358.738
3	2942.855	3525.691
4	5519.541	6511.161
5	3399.978	4015.697
6	2519.028	2966.141
7	2218.973	2559.236

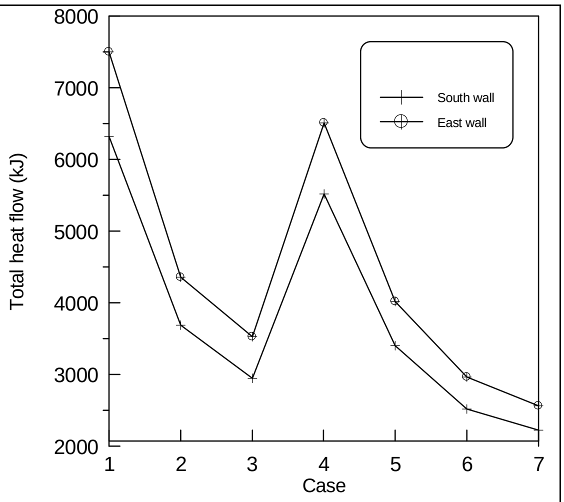

Figure (23) Total heat flow